

Influence of Low Permeability Capping Layers on Liquefaction Induced Failure in Stratified Ground



Divyesh Rohit, Siavash Manafi Khajeh Pasha, Hemanta Hazarika, Takaji Kokusho, and Sukiman Nurdin

Abstract Large-scale permanent ground deformations due to an earthquake are generally termed as flow liquefaction (FL). Flow failures are often observed in gentle slopes where minimum undrained shear strength remains less than static shear stress even after ground motion ceases and the induced deformations continue until a balance is achieved. Such failures are caused by significant strength loss in saturated granular soils due to the seismic induced excess pore water pressure (PWP). As the soil strength is reduced, plastic deformations can occur even due to static shear stresses such as building loads or driving forces on sloping ground. While such deformations are rare in level grounds with saturated sandy deposits, the triggering of such events depends on the ability of soil in retardation of dissipation of excess PWP which controls the effective stress in the layer. The dissipation of PWP is influenced by the permeability of interlayers in the layered sand deposit. As in natural conditions, sand deposits are highly heterogeneous and stratified, they often tend to contain low permeability capping layers sandwiched between them. This low permeability tends to inhibit the dissipation of PWP after the onset of ground shaking, which leads to further instability of overlying layer. This study aims to investigate the effect of such capping layers on the PWP dissipation and deformation of saturated sand deposits under dynamic loading conditions. To evaluate the buildup and dissipation

D. Rohit (✉) · S. M. K. Pasha · H. Hazarika
Kyushu University, Fukuoka 819-0395, Japan
e-mail: rohit.divyesh@gmail.com

S. M. K. Pasha
e-mail: manafi.siavash@gmail.com

H. Hazarika
e-mail: hazarika@civil.kyushu-u.ac.jp

T. Kokusho
Chuo University, Tokyo 192-0393, Japan
e-mail: koktak@ad.email.ne.jp

S. Nurdin
Tadulako University, Palu 94148, Indonesia
e-mail: s.nurdin@gmail.com

of PWP in a simple way, multiple one-dimensional (1D) model tests were conducted by imparting dynamic loading to a soil column with different capping layer conditions. Multiple parametric studies were conducted with varying relative density of sandwiching layer, capping layer thickness, and capping layer material.

Keywords Flow liquefaction · Capping layer · Excess pore water pressure · Settlement

1 Introduction

1.1 Background

The liquefaction resistance of a site does not merely depend on the soil deposits but also on the heterogeneity of stratification. Typically, in case of gently sloped alluvium deposits, the liquefaction susceptibility depends not only on the shear strength of deposits but also on the permeability characteristics of the soil interlayers which may have a low permeability coefficient. The permeability of these sandwiched layers is of key importance as they control the dissipation of excess pore water pressure (EPWP) which develops in saturated deposits during shear wave propagation. During liquefaction in a saturated sand deposit, the excess pore water developed dissipates through the overlying deposits to the ground, thereby carrying sand and fines along with it creating sand boils [16]. With the expulsion of pore water, the soil particles get packed densely causing settlements.

In past most disastrous damages due to seismically developed EPWP have occurred in inclined ground, earthen dam structures and dikes where a possible failure surface already exists prior to the impact of seismic wave [16]. The failure surface in these types of liquefactions is usually large and causes massive soil displacement, called flow failure. The flow failures are mainly triggered by gravitational forces under static condition which occurs when the strength of soil reduces to strength required for static stability conditions [9]. While such large-scale flow failures are expected to occur in ground with higher gradients, in past earthquakes the flow or movement of soil mass has been observed to be upto several meters even in ground of a very low gradient [3]. Although liquefaction at sites with no or a very gentle slope is considered to be a simple phenomenon, the mechanisms involved in initiation of liquefaction like the buildup and dissipation of pore water pressure are quit complex [16].

Such type of flow failure has been observed during the 1964, Niigata earthquake where a considerable ground movement was observed for a ground surface with gentle slope of less than 1% [3]. Further, such failures also seem to occur after the cease of ground motion as observed during past events [2, 1]. These case histories imply that for a gentle slope to undergo flow failure, not only gravity but other multiple mechanisms are required to trigger the failure [6]. While the exact mechanism of such failures in level grounds is not known, previous researchers have attributed the

cause to the presence of impermeable layer sandwiched between permeable sand layers. These interlayers inhibit the dissipation of EPWP due to low permeability, thereby stopping the liquefied soil layers to stabilize after the onset of liquefaction [5–8].

The current research aims in studying large-scale flow liquefaction observed on a ground with very gentle slope during the recent 2018, Sulawesi earthquake event where the ground displacement from few meters to about several hundred meters was observed killing thousands of people and devastating many villages during the event. The city of Palu, which lies in the Central Sulawesi Province of Indonesia, witnessed massive flow liquefaction during the September 28, 2018, earthquake of magnitude M_w 7.5 epicentered in the Minahasa Peninsula neck.

1.2 Site Geology and Seismic History

The city of Palu lies in the Central Sulawesi Province in Sulawesi Island of Indonesia. The city is straddled by a seismically active sinistral Palu—Koro fault which has an annual tectonic slip rate of around 40 mm [11]. The region is overlain by sedimentary and volcanic deposits of Miocene—Quaternary period, which have undergone low grade thermal metamorphism [15]. The Palu Valley extends to 7 km in width and flanked by N-S aligned, around 60 m high sharp triangular slopes and short alluvial fans in West, and gently steps faults in East [13]. Hosting an active strike—slip fault, the region has experienced multiple large devastating earthquakes in the past. Historic seismicity of the PKF region shows that the fault activity is concentrated at shallow depth with major earthquakes of magnitude $M_w \geq 6.5$ during years 1900–2018 have a hypocentral depth of less than 50 m [11, 14] as shown in Fig. 1a and b. Where

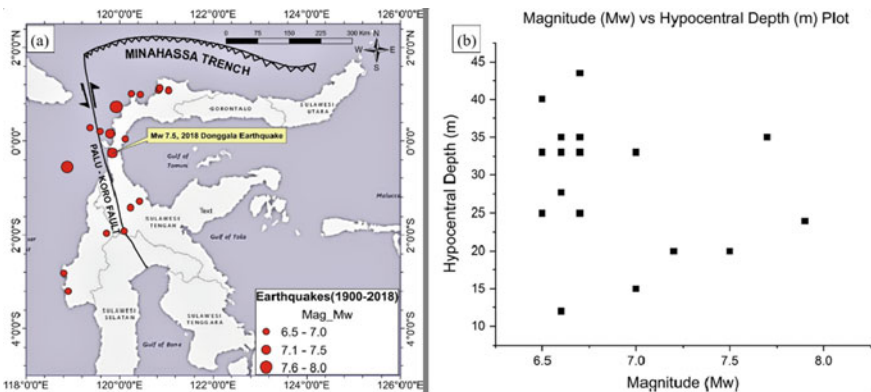


Fig. 1 a Earthquakes across PKF with magnitude $M_w \geq 6.5$ during years 1900–2018 and b Plot of magnitude (M_w) versus Hypocentral depth (m) for the same events [11, 14]

Fig. 1a shows the major seismic activity of PKF for period 1900–2018, and Fig. 1b shows the plot of magnitude (M_w) to hypocentral depth.

2 Case Study

2.1 Event History

On September 28, 2018, Central Sulawesi was struck by a powerful earthquake of magnitude M_w 7.5 with strong foreshocks and aftershocks for multiple days. The event occurred as a result of strike—slip faulting at a shallow depth. The seismic waves produced by the earthquake at hypocenter of 20 km [14] caused large-scale liquefaction and flow failures across multiple locations in the city of Palu. Even though the distance from epicenter was around 70 km, most damage was observed in Jono Oge, Sibalaya, and Balaroa villages in Sigi Regency in Palu [4]. The foreshock, mainshock, and aftershock map of the event is shown in Fig. 2. The event had a major foreshock of magnitude M_w 6.1 just three hours before the mainshock and several aftershocks of magnitude $M_w \geq 5.5$, which shows that large amount of elastic strain energy had been accumulated in the fault [14].

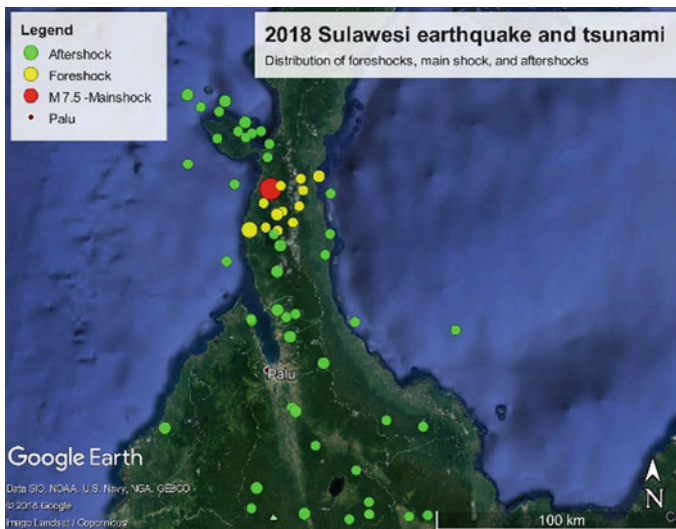


Fig. 2 Distribution of foreshock, mainshock and aftershock for 2018 Sulawesi earthquake (modified from USGS [14])

2.2 Site Investigation

Our team from Kyushu University visited the flow liquefaction sites in Jono Oge, Sibalaya, and Balaroa in Palu aftermath of earthquake. The survey elements included site reconnaissance, disturbed soil sampling, portable dynamic cone penetration tests (PDCPT) and aerial survey with drone. Figure 3 here depicts the condition of the flow failure site at Jono Oge before (Fig. 3a) and after the seismic event (Fig. 3b). The site mainly composed of agricultural fields with a scant population and a very gentle sloping ground of less than 2% (Fig. 3c). It was also found that an irrigation channel which was passing from the eastern side of failure zone breached due to the liquefaction during the shockwave propagation as shown in Fig. 3b. Due to the presence of irrigation channel, the ground water level was very high (<5 m from ground surface) which is also considered to be a key factor contributing to flow failure. The breach of water channel discharged a large volume of water into the already failed zone causing a massive mudflow as shown in Fig. 3b.

The maximum site amplification occurred in the Palu Valley, which has deposits with low shear wave velocity profile [10], as can be seen in Fig. 4a. It can be seen that the valley region along with the coast line has very low shear wave velocity while the mountainous region has high V_{s30} values. Figure 4b depicts the satellite image of liquefaction site at Balaroa before the event while Fig. 4c shows the condition of the site after liquefaction taken by a drone camera. It can be ascertained from Fig. 4b and c that a large-scale liquefaction occurred devastating and displacing all the housing structures in the area to hundreds of meters.

Further in Fig. 5a shows the location where the PDCPT and SPT tests were performed at the flow failure site in Jono Oge. Figure 5b shows the condition of soil profile at crown of failure, also depicting the difference in elevation of ground after liquefaction. Figure 5c represents the plot of N values versus depth obtained from

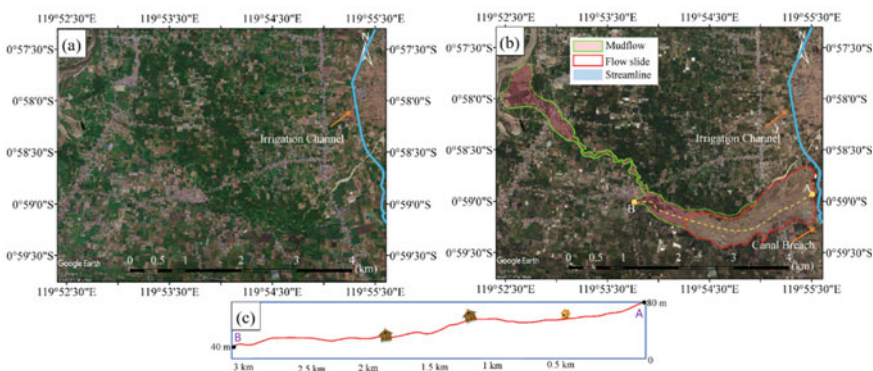


Fig. 3 Lateral flow area in Jono Oge village due to Sulawesi Earthquake, **a** before flow failure, **b** after flow failure with mud flow and water channel and **c** slope profile of the flow area (modified from Google Earth)

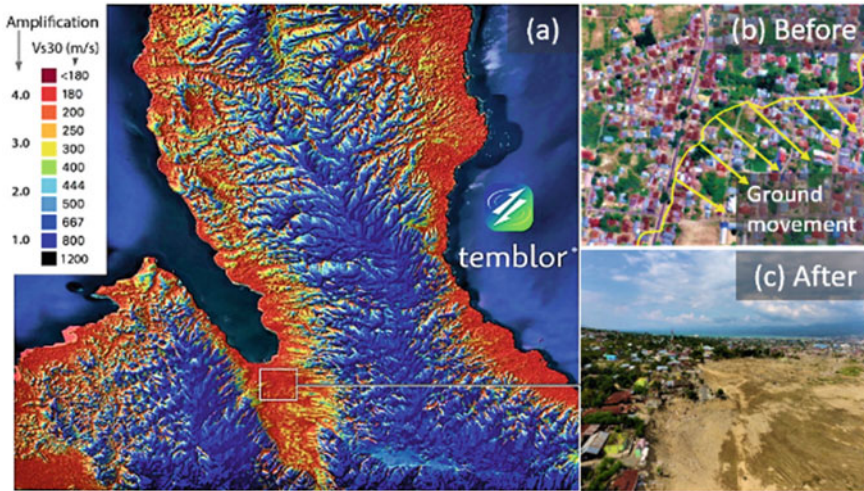


Fig. 4 Vs30 map of Palu region along with a site amplification forecast for an Mw 7.5 earthquake [10], **b** Google Earth image for site in Balaroa, Palu, prior to 2018, Sulawesi Earthquake and **c** Drone Image of Balaroa site after the event showing mass displacement of structures from original location

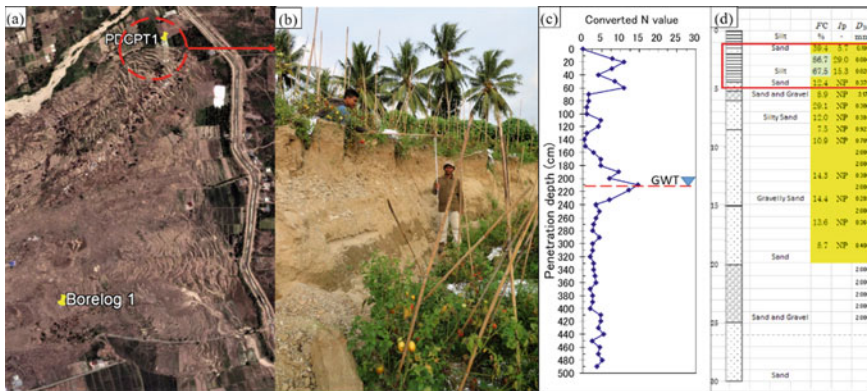
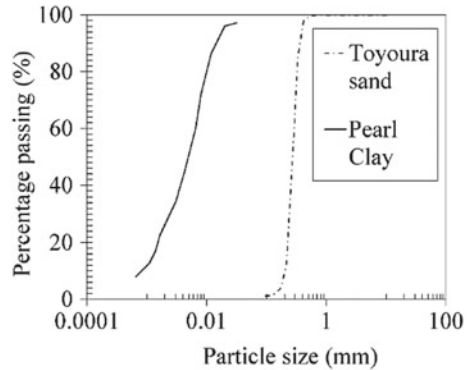


Fig. 5 **a** Location of PDCPT and SPT at Jono Oge, **b** Location of crown of the flow failure at Jono Oge site with high vertical settlement, **c** plot of N-value versus depth obtained by PDCPT1 test outside the failure zone and **d** Borelog1 profile of soil in failure zone

PDCPT test conducted outside the crown of failure zone. It can be seen from the plot that the subsoil condition is weak with a maximum *N*-value reaching upto 15 and dropping back to low numbers and presence of water table at a shallow depth of 2.15 m from the ground surface. Further Fig. 5d shows the subsoil condition at location of Borelog 1. It can be seen from the illustration that the silt layers are sandwiched in between sand layers at shallow depth with a higher fines content and some plasticity characteristics. These soft sandwiched silt layers are considered to

Fig. 6 Gradation curve for Toyoura sand and Pearl clay



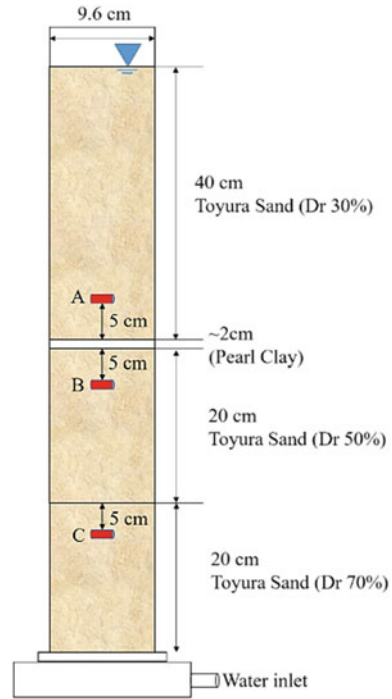
be a probable contributor to the large-scale flow failure by inhibiting the dissipation EPWP from below sand and gravel layers.

2.3 1-D Model Tests

To evaluate the effect of a low permeability sandwiched soil layer between sand or gravel layers and understand the mechanism of lateral flow at Jono Oge, 1D model tests were conducted in laboratory by trying to mimic the soil stratification conditions in which a silt or clay seam is sandwiched between sand layers. In the current study, 1D model tests were conducted using loose saturated Toyoura sand with a seam Pearl clay sandwiched between the sand layers. Pearl clay which has 50% clay and 50% silt content was used as a capping layer to simulate the presence of a silt seam or clay layer in field and evaluate its effect on the dissipation of excess pore water pressure. The grain size distribution of Toyoura sand and Pearl clay is given in Fig. 6. The Toyoura sand has specific gravity, G_s is 2.65 and maximum (e_{max}) and minimum (e_{min}) void ratios of 0.977 and 0.615, respectively. For Pearl clay, the G_s is 2.71 and the liquid limit and plasticity index are 49% and 27%, respectively [12]. The schematic experimental setup of 1D test is given in Fig. 7.

As shown in Fig. 7, the D_r is the relative density of the sand layer. A, B, and C are the pore water transducers. A condition of liquefaction was generated by providing a shock through a hammer blow to the 1D setup at the base. The resulting excess pore water pressures were measured and analyzed for conditions with clay seam and without clay seam.

Fig. 7 Schematic diagram of 1D experimental setup



3 Results and Discussions

The results for 1D model test after a single impact of hammer are plotted as the ratio of excess pore water pressure to maximum excess pore water pressure (u/u_{max}) versus time (s). The u/u_{max} value has been plotted against the duration to show the effect of clay seam on development and dissipation of excess pore water pressure in saturated sand under impact loading. Figure 8 shows the plot for condition with no clay seam present (Case 1). Here in Fig. 8 it can be seen that the EPWP developed for pore water transducer C is higher than A and B. This may be due to its location at the bottom from where the dissipation of EPWP takes time, while at A the EPWP is dissipated quickly since it is near to surface. Further, at B, the EPWP is developed but gets dissipated quicker than at C due to shorter seepage path. Further in Fig. 9, the plot for case for clay seam sandwiched between sand layers is shown (Case 2). Here, the EPWP developed at pore water transducer B is highest due to presence of clay seam above which inhibits the dissipation of EPWP. It can also be observed that the EPEP at A is higher than at C which may be attributed due to a higher relative density at the bottom during sample preparation.

Further in Fig. 10, the plot for u/u_{max} versus time for transducer B is compared for both the cases (1 and 2). From the figure, it can be observed that ratio u/u_{max} for B (2) takes longer duration to dissipate after reaching peak and still has a higher

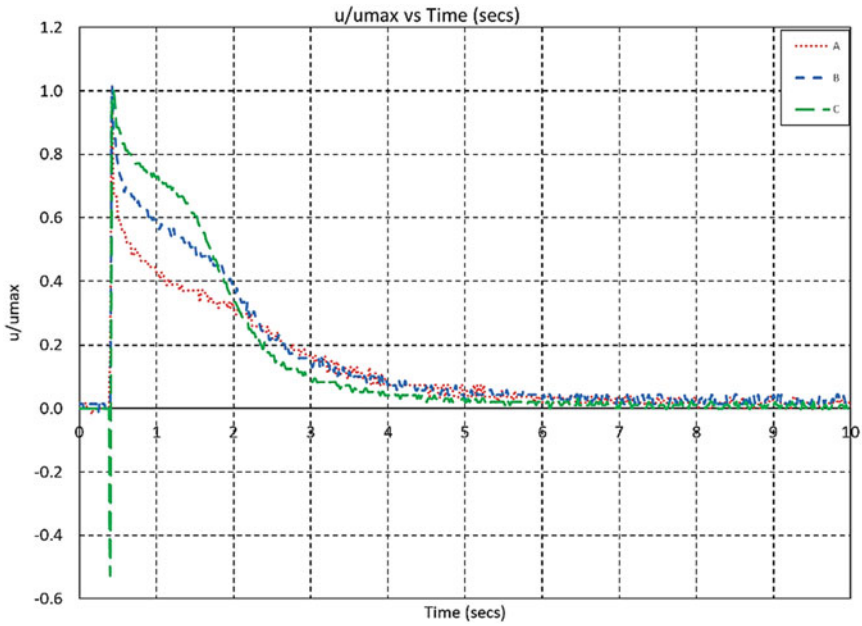


Fig. 8 Plot of u/u_{max} versus time (s) for Case 1 with pore water transducers at three locations across the height

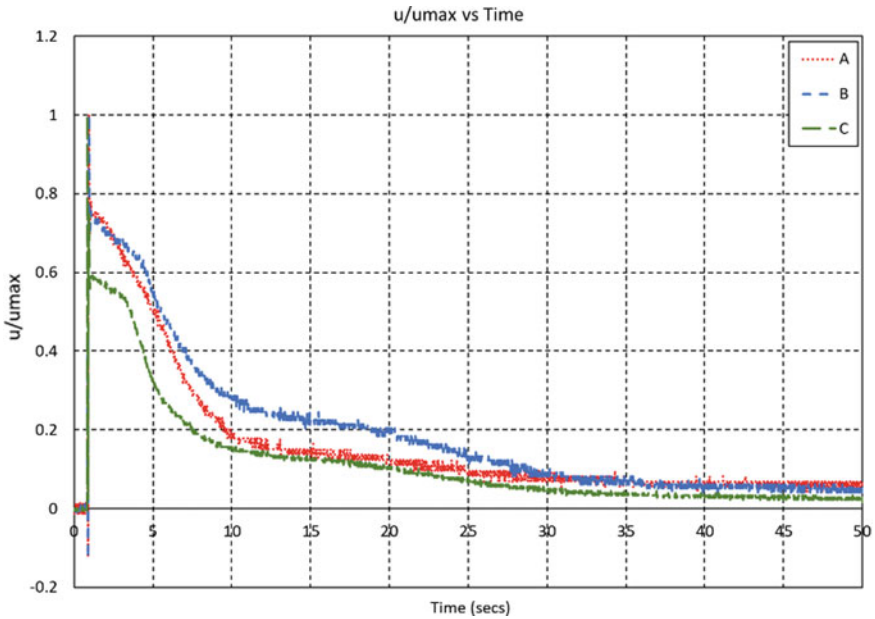


Fig. 9 Plot of u/u_{max} versus time (s) for Case 2 with pore water transducers at three locations across the height

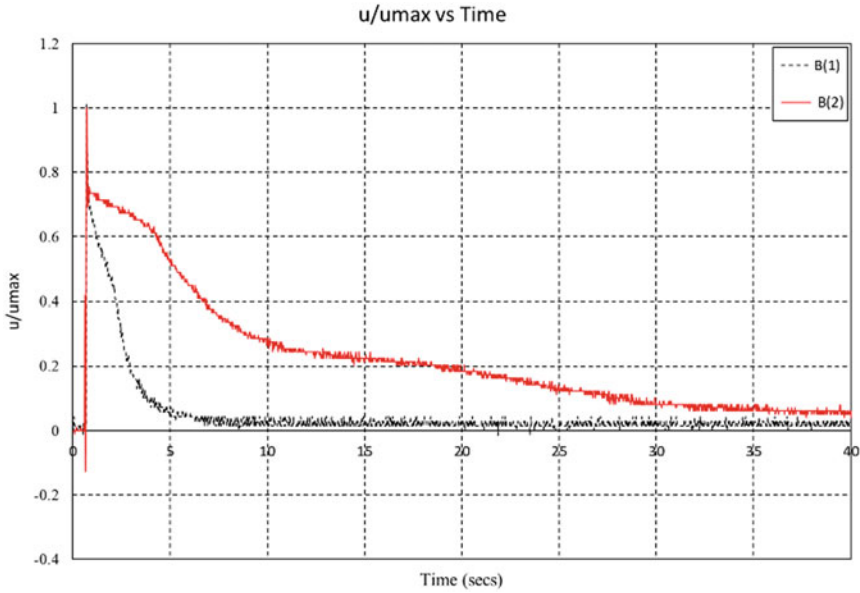


Fig. 10 Dissipation of excess pore water pressure versus time (s) at pore pressure transducer B for Cases 1 and 2

value while that for B (1) is dissipated. This implies the capping effect of clay seam which prevents the dissipation of excess pore water pressure in the sand layer below. In Fig. 11, the plots for u/u_{max} versus time for pore pressure transducers A and C are shown, where A is located above the clay seam and C is located at a distance of 15 cm from the bottom of the sand layer with D_r 70%. Here for both the transducers, the duration for dissipation of excess pore water pressure for sand with clay seam is higher than the condition without clay seam. This shows that the presence of a low permeability layer cannot only hinder the dissipation of pore water pressure in adjacent areas but also in regions at a higher distance from the layer vertically.

The pictorial evidence of the effect of clay seam in sand layer during liquefaction can be seen in Fig. 12. Here the development of water layer below the clay seam at different time frames is shown. Figure 12a is recorded at $T = t$ s when the hammer impact was made. Figure 12b depicts the maximum thickness of the water film at $t + 5$ s while Fig. 12c shows the decreased water film thickness at $t + 35$ s. This shows how the water film dissipates slowly, thereby influencing the dissipation of excess pore water pressure from the below sand layers by forming an impermeable capping layer. The water film thus created causes settlements in the clay seam after the overall dissipation of EPWP which can be seen in Fig. 13. Here in Fig. 13a, the base of clay seam can be seen at 39.8 cm which settles to 39.0 cm after the hammer blow due to the liquefaction as shown in Fig. 13b.

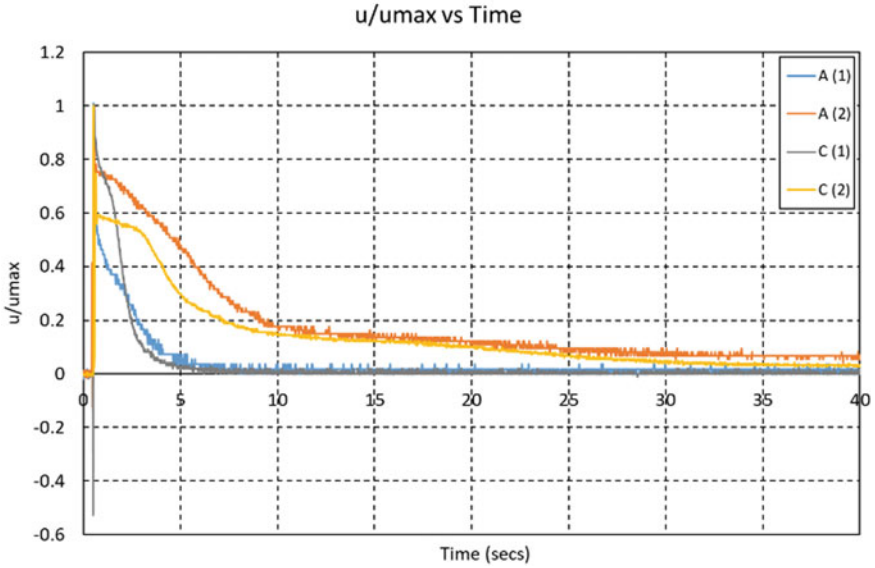


Fig. 11 Dissipation of excess pore water pressure versus time (s) at pore pressure transducers A and C for Cases 1 and 2

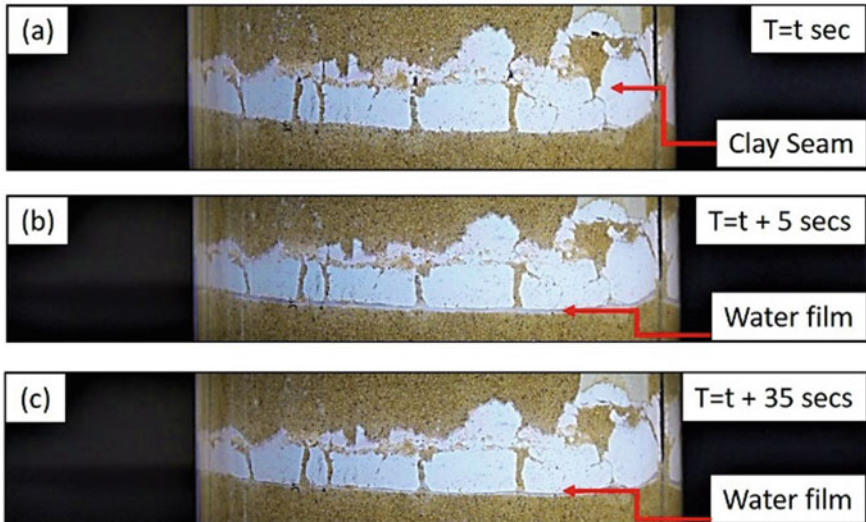


Fig. 12 Formation of water layer under the clay seam at different time durations: **a** Time (T) = t s, **b** $T = t + 5$ s and **c** $T = t + 35$ s

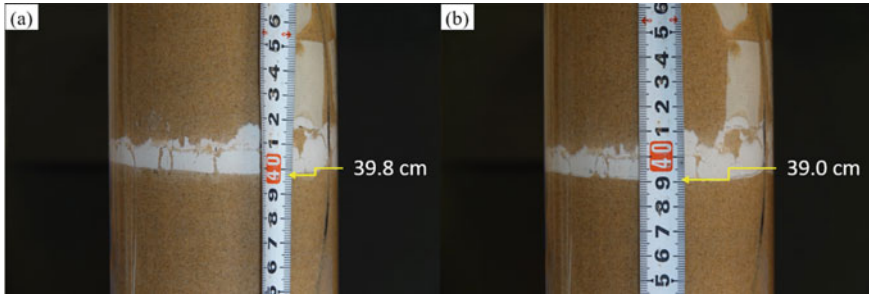


Fig. 13 Height of clay seam **a** before liquefaction and **b** after liquefaction

4 Conclusion

The team of authors conducted site investigation at Jono Oge, Sibalaya and Balaroa villages in Palu, Indonesia, after the September 2018, Sulawesi earthquake which caused large loss of life as well as massive damage to infrastructure. Multiple field tests including PDCPT and aerial drone photography were conducted. From the field tests, it was observed that sandy soil consists of silt layers with some clay content sandwiched in between sand and gravel layers. 1D model tests were conducted to ascertain the cause of flow failure by simulating the site conditions as per the observations of field investigations. From the results of 1D model tests, it was observed that the presence of a low permeability silt or clay seam sandwiched between saturated sand layers can inhibit the dissipation of excess pore water pressure due to the impact of dynamic loading. This delay in turn causes the reduction in residual strength of soil to the static shear stress, which can cause further instability in the top layer by causing excessive settlements and flow failure. Although liquefaction is a complex phenomenon involving multiple parameters, the authors conclude that the presence of such low permeability silt or clay layers can act as one of the major contributing factor in flow failure.

References

1. Berrillj, B.: Lateral spreading loads on a piled bridge foundation, seismic behavior of ground and geotechnical structures. Proc. Spec. Tech. Sess. Earthq. Geotech. Eng. ICSMGE Hambg., 153–183 (1997)
2. Bolton, S.H.: Design problems in soil liquefaction. *J. Geotech. Eng.* **113**(8), 827–845 (1987)
3. Hamada, M.: Large ground deformations and their effects on lifelines : 1964 Niigata earthquake, Case Studies of Liquefaction and Lifeline Performance during Past Earthquakes. *Japanese Case Stud.* **1**, 3.1–3.123 (1992)
4. Hazarika, H., Rohit, D., Pasha, S.M.K., Maeda, T., Masyhur, I., Arsyad, A., Nurdin, S.: Large distance flow-slide at Jono-Oge due to the 2018 Sulawesi Earthquake, Indonesia. *Soils Found.* **61**(1), 239–255 (2020)

5. Kokusho, T.: Water film in liquefied sand and its effect on lateral spread. *J. Geotech. Geoenviron. Eng.* **125**(10), 817–826 (1999)
6. Kokusho, T.: Mechanism for water film generation and lateral flow in liquefied sand layer. *Soils Found.* **40**(5), 99–111 (2000)
7. Kokusho, T., Fujita, K.: Site investigations for involvement of water films in lateral flow in liquefied ground. *J. Geotech. Geoenviron. Eng.* **128**(November), 917–925 (2002)
8. Kokusho, T., Kojima, T.: Mechanism for post liquefaction water film generation in layered sand. *J. Geotech. Geoenviron. Eng.* **128**(2), 129–137 (2002)
9. Kramer, S.L.: *Geotechnical Earthquake Engineering*: Pearson New, International edn. Pearson Education Limited, New Jersey (2013)
10. Patton, J.R., Stein, R., Sevilgen, V.: Coseismic landslides in Sulawesi, Indonesia. [Online]. Available: <http://temblor.net/earthquake-insights/coseismic-landslides-in-sulawesi-indonesia-7874/>. Accessed: 26 Feb 2019
11. Socquet, A., Simons, W., Vigny, C., McCaffrey, R., Subarya, C., Sarsito, D., Ambrosius, B., Spakman, W.: Microblock rotations and fault coupling in SE Asia triple junction (Sulawesi, Indonesia) from GPS and earthquake slip vector data. *J. Geophys. Res.* **111**, B08409 (2006). <https://doi.org/10.1029/2005JB003963>
12. Sun, D.A., Matsuoka, H., Xu, Y.F.: Collapse behavior of compacted clays in suction-controlled triaxial tests. *Geotech. Test. J.* **27**(4), 362–370 (2004)
13. Theinab, P.S., Pramumijoyob, S., Brotopuspitoc, K.S., Kiyonod, J., Wilopob, W., Furukawad, A., Setiantob, A., Putra R.R.: Estimation of S-wave velocity structure for sedimentary layered media using microtremor array measurements in Palu City, Indonesia. *Procedia Environ. Sci.*, vol. 28, no. SustaiN 2014, pp. 595–605 (2015)
14. USGS: United States Geological Survey. 2018. [Online]. Available: <https://www.usgs.gov/>. Accessed: 14 Jul 2019
15. van Leeuwen, T., Allen, C.M., Elburg, M., Massonne, H.J., Palin, J.M., Hennig, J.: The palu metamorphic complex, NW Sulawesi, Indonesia: origin and evolution of a young metamorphic terrane with links to Gondwana and Sundaland. *J. Asian Earth Sci.* **115**, 133–152 (2016)
16. Vucetic, M., Dobry R.: Pore pressure build-up and liquefaction at level sandy sites during earthquakes. Rensselaer Polytechnic Institute Research Report. CE-86–3, (1986)